

# SHAPE MEMORY POLYMER COMPOSITE AND ITS APPLICATION TO DEPLOYABLE HINGE FOR SOLAR ARRAYS

JS. Leng\*, XH. Wang, X. Lan, YJ. Liu

Harbin Institute of Technology, China

P.O. Box 3011, Centre for Composite Materials and Structures, No. 2 YiKuang Street, Science Park of Harbin Institute of Technology (HIT), Harbin 150080, P.R. China

## ABSTRACT

This paper is concerned about the basic properties of deployment of shape memory polymer composite (SMPC) and its application to deployable hinge for solar arrays. Shape memory polymer (SMP) used in this study is a thermoset styrene-based shape memory resin in contrast to normal thermoplastic SMPs. Carbon fiber fabric reinforced SMPC is discussed here. In order to investigate the basic performances of deployment for SMPC hinge, the experimental methods are used as follows: dynamic mechanical analysis (DMA), three point bending test and deployment tests. Results indicate that the glass transition temperature ( $T_g$ ) of SMPC is approximate 63°C. SMPC shows typical linear elasticity and high bending modulus before glass transition in SMP, while exhibits apparent nonlinear viscoelasticity and low bending modulus within the range of glass transition in SMP. The shape recovery ratio of SMPC is above 90% at/above  $T_g$ , while drops sharply at below  $T_g$ . The deployment properties of SMPC depend strongly on the number of thermomechanical cycles, which become relatively stable after some packaging/deployment cycles. Moreover, deployment velocity and shape recovery ratio rise remarkably with the increase of temperature of SMPC, while they increase in a weak trend with the increase of pre-deformation temperature. In the end, a prototype of solar array actuated by SMPC hinge, which is heated by passing an electrical current, deploys from about 180° to 0° in one minute. This SMPC hinge performs good deployment performances during numerous thermomechanical cycles.

**Keywords:** shape memory polymer, carbon fiber fabric composite, deployable hinge, solar arrays

## 1. INTRODUCTIONS

Shape memory polymer (SMP) is a typical kind of smart material, which presents high strain capacity (an order of 100% reversible strains), low density and low cost etc [1-3]. But the primary drawbacks of pure SMP are low strength, low modulus and low recovery stress [4-5]. Consequently the fiber reinforced shape memory polymer composite (SMPC) is naturally considered to be manufactured [6-7]. With the characteristics of high reversible strain, high strength, high modulus and relatively high recovery stress, SMPC develops substantial interest to be used for the actuators for the deployable structures, such as deployable space antenna, truss and solar arrays in space industry and other applications [8-10]. Comparing with existing actuators of solar arrays,

there are no moving parts in the deployable system. Thus the deployable SMPC hinge simplifies deployment structure and subsequently decreases its mass. As the stiffness of SMPC below  $T_g$  is as high as usual polymer-based composite, the constraint devices is not needed in deployment system during the process of launching. Moreover, as the motion of SMPC hinge is only stimulated by the behavior of glass transition in SMP, release devices can be eliminated in deployment system.

In this study, we develop a novel type of fiber reinforced styrene-based SMPC hinge for the actuation of deployment for solar arrays. Our focuses are: Influence of fiber reinforcement on glass transition of SMPC; Influence of temperature on bending modulus of SMPC; deployment properties upon bending of SMPC; deployment sequence of a prototype of solar array actuated by SMPC hinge (see Fig. 1).

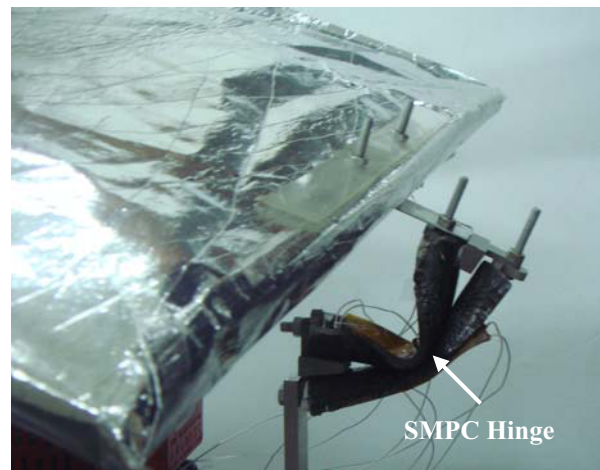


Fig.1 A prototype of solar array actuated by SMPC hinge

## 2. EXPERIMENTAL METHODS

Carbon fiber fabric was used to reinforce a thermoset styrene-based SMP. The SMPC was fabricated by the standard fabrication techniques for fiber reinforced composite materials, i.e., curing of a pre-impregnated fabric. The SMPC was reinforced by 3-ply plain weaves. For comparison, pure SMP specimen was cured under the same conditions as that of SMPC.

In order to investigate the basic thermomechanical performances of SMPC at different temperatures, a dynamic mechanical analyzer (NETZSCH, DMA242C) was

\* Lengjs@hit.edu.cn; phone +86-(0)451-86402328; fax +86-(0)451-86402328

used for a dynamic thermal scan to determine the storage modulus and tangent delta. Three-point bending mode was applied with a span of 40 mm. The dimensions of specimens were 50×9×3 mm. The scanning range of temperature was 0–120°C at a heating rate of 2°C/min and a frequency of 1 Hz.

Instron 5569 test machine was used to investigate the basic mechanical properties of SMPC with a setup of three-point bending. The dimensions of specimens were thickness 3 mm, width 15 mm and gauge length 30 mm. The speed of crosshead was set as 2 mm/min. A thermostatic chamber (EUROTHERM 2408) was used to control the environmental temperature.

Shape recovery test upon bending was discussed in detail to investigate the basic deployment performances of SMPC in a water bath, which was a prerequisite for the application of SMPC hinge to solar arrays.

In the end, a prototype of SMPC hinge was heated by passing an electrical current through surface-bonded heaters to simply evaluate the actuation properties for the deployment of solar arrays.

### 3. EXPERIMENTAL RESULTS AND DISCUSSIONS

#### 3.1. Dynamic mechanical analysis of SMPC

The curves of storage modulus and tangent delta versus temperature for pure SMP and SMPC are plotted in Fig. 2. According to the curves of storage modulus, it is clear that SMPC has a higher storage modulus than that of pure SMP. The storage modulus of SMPC falls precipitously within the glass transition region of about 40–80°C (from  $T_g-20^\circ\text{C}$  to  $T_g+20^\circ\text{C}$ ). The peak value of tangent delta is defined as the glass transition temperature ( $T_g$ ). Hence, the  $T_g$  of pure SMP and SMPC is found to be about 54°C and 64°C, respectively. It is obvious that the  $T_g$  of SMPC is higher than that of pure SMP, which is due to the effect of fiber reinforcement.

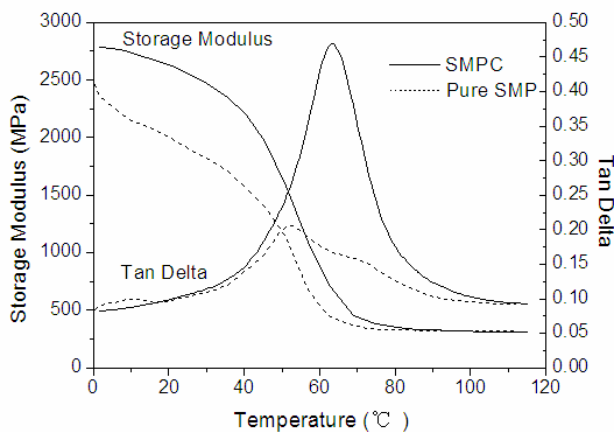


Fig. 2 Curves of storage modulus and tangent delta versus temperature of pure SMP and SMPC

#### 3.2. Three-point bending test of SMPC

In order to compare the basic mechanical properties of SMPC at different temperatures, three-point bending test was performed. Fig. 3 shows the relationship between load and deflection at some different temperatures ( $T_g-40^\circ\text{C}$ ,  $T_g-20^\circ\text{C}$ ,  $T_g-10^\circ\text{C}$ ,  $T_g$ ,  $T_g+10^\circ\text{C}$ ). The resultant bending modulus at different temperatures are shown in Fig. 4. The bending modulus falls remarkably with the increases of temperature associated with the softening effect due to glass transition. At  $T_g-40^\circ\text{C}$ , SMPC exhibits the highest bending modulus than the others. In addition, at  $T_g-40^\circ\text{C}$ , the load increased linearly to about 125.0 N with the deflection of 1.70 mm, while keeps relatively constant beyond this point. On the other hand, there is no significant linear region at testing temperatures of  $T_g-20^\circ\text{C}$ ,  $T_g-10^\circ\text{C}$ ,  $T_g$  and  $T_g+10^\circ\text{C}$ . It is noticed that, SMPC exhibits nonlinear viscoelastic response from  $T_g-20^\circ\text{C}$  that is the starting temperature of glass transition (see Fig. 2). At  $T_g-10^\circ\text{C}$ , the bending modulus becomes very low due to further glass transition. At  $T_g$  and  $T_g+10^\circ\text{C}$ , the 'soft' SMP (glassy state) shows weak resistance against the applied external force.

It can be found that SMPC shows typical linear elasticity and high bending modulus before the glass transition, while exhibits apparently nonlinear viscoelasticity and low bending modulus upon the appearance of glass transition. Additionally, the results of static mechanical test coincide well with these of dynamic mechanical analysis.

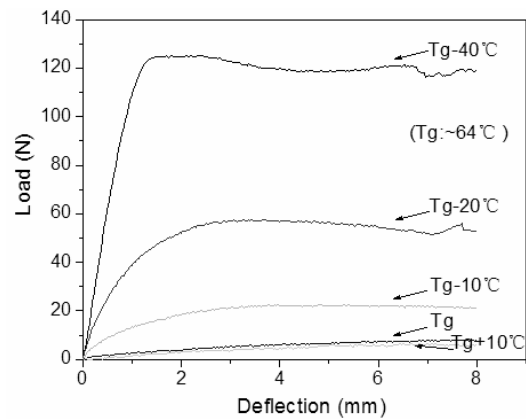


Fig. 3 Curves of load versus deflection in three-point bending

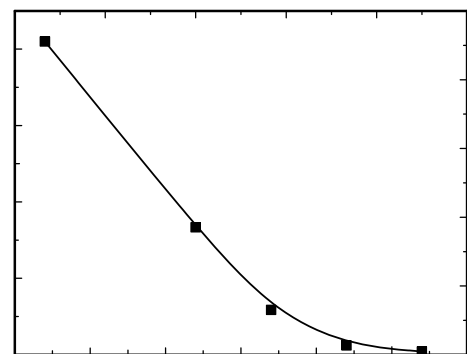


Fig. 4 Curves of bending modulus versus temperature in three-point bending

### 3.3. Deployment performances of SMPC

Bending test is conducted to investigate the bending recovery performances of SMPC. The method which is used to quantify the precision of deployment is illustrated in Fig. 5, where,  $r$  denotes the radius of mandrel,  $t$  represents the thickness of SMPC specimen,  $\theta_0$  is a certain original bent angle that is selected for testing,  $S(x_0, y_0)$  is a point selected to determine  $\theta_0$ ,  $\theta_N$  is the residual angle of the Nth thermomechanical bending cycle.  $R(x_N, y_N)$  is a testing point in order to calculate  $\theta_N$ :

$$\theta_N = \cot^{-1} \left( \frac{x_N}{y_N} \right) \quad (N = 1, 2, 3, \dots) \quad (1)$$

The value of shape recovery ratio is calculated by:

$$R_N = \frac{\theta_0 - \theta_N}{\theta_0} \times 100\% \quad (N = 1, 2, 3, \dots), \quad (2)$$

where,

$R_N$  denotes the shape recovery ratio of the Nth thermomechanical bending cycle.

The procedure of thermomechanical bending cycling of SMPC includes the following steps: (1) Specimen is kept in water bath for 5 minutes at  $T_g + 20^\circ\text{C}$  (original shape); (2) The SMPC is bent to a certain angle around a mandrel with the radius of 2 mm in the soft rubbery state (pre-deformation); (3) The SMPC is kept in cool water with the external constraint to “freeze” the elastic deformation energy for 5 minutes (storage); (4) The SMPC specimen that is fixed on the apparatus is immersed into another water bath at a certain elevated temperature, and then it recovers to a certain residual angle (recovery). Then,  $R(x_N, y_N)$  is measured by a vernier caliper with a resolution of 0.01 mm. Finally,  $\theta_N$  and  $R_N$  are obtained through Equations 1 and 2.

We know that carbon fiber's tensile stiffness is much higher than its compressive stiffness and the stiffness of SMP matrix at high temperature. Hence, we assume that, during bending, the neutral axis moves from the middle layer of specimen towards the outer surface where fibers are in a tensile strain state<sup>7</sup>. Subsequently, the traditional assumption in simple beam theory (Gere and Timoshenko, 1990) can be applied here. Based on the assumption of linear distribution of compressive strain along the thickness of specimen, one has:

$$\frac{r}{t} = \frac{1}{\varepsilon}, \quad (3)$$

where  $\varepsilon$  is the maximum strain on the inner surface where we assume the strain on the outer surface to be zero.

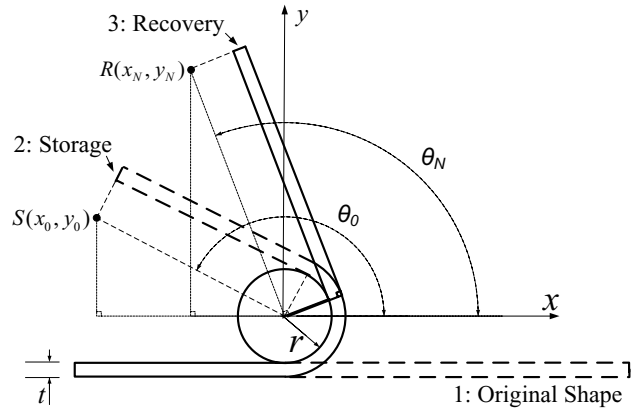


Fig. 5 Schematic illustration of deployment performances test

#### 3.3.1. Deployment performances at different temperatures

In order to investigate the deployment rate and deployment ratio of SMPC at different temperatures, the test of position versus time was conducted at some different temperatures, namely  $T_g - 20^\circ\text{C}$ ,  $T_g - 10^\circ\text{C}$ ,  $T_g$ ,  $T_g + 10^\circ\text{C}$ . The temperature of pre-deformation of SMPC was set as  $T_g$  of SMPC ( $64^\circ\text{C}$ ). The original bent angle was selected as  $180^\circ$ .

Fig. 6 shows the relationship between position and time in a deployment process during the first 140 seconds. It reveals that, SMPC specimen deploys relatively faster at higher temperature in initial stage. At/Above  $T_g$ , SMPC specimen deploys fast in initial stage, then deployment velocity will lower quickly at a certain temperature associated with a fast glass transition of SMP. Below  $T_g$ , SMPC specimen deploys very slow due to a process of a part of glass transition. In a word, it achieves an equilibrium state faster with the increase of temperature. In additionally, as shown in Fig. 7, at above  $T_g$  the deployment ratio against temperature shows a weak rising trend. The deployment behavior can also be observed within the range of  $T_g - 20^\circ\text{C}$  to  $T_g$ , which demonstrates that the glass transition occurs in a continuous region ( $T_g - 20^\circ\text{C}$  to  $T_g + 20^\circ\text{C}$ , see Fig. 2). However, the shape recovery ratio drops sharply within this temperature range due to a relatively high stiffness of SMPC at an original stage of glass transition.

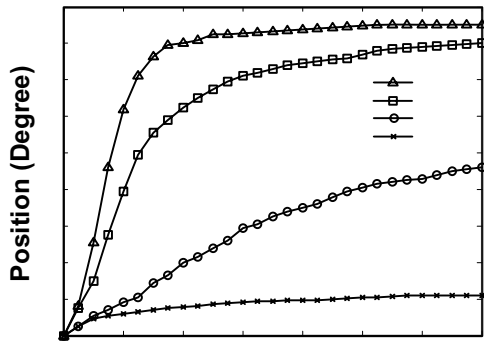


Fig. 6 Relationship between position and time of shape recovery at different temperatures

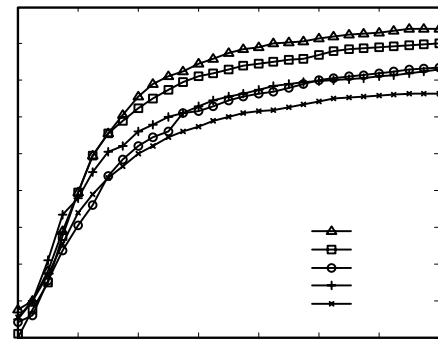


Fig. 8 Relationship between position and time of shape recovery at different pre-deformation temperatures

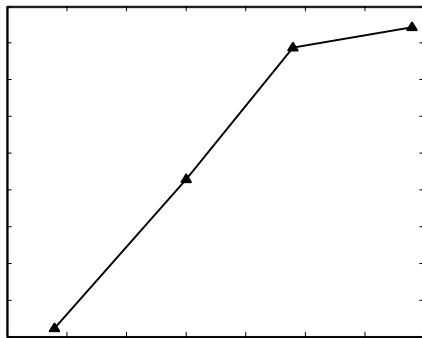


Fig. 7 Shape recovery ratio at different temperatures

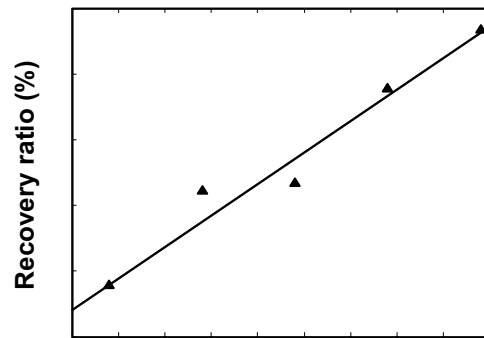


Fig. 9 Shape recovery ratio versus pre-deformation temperatures

### 3.3.2. Deployment performances at different pre-deformation temperatures

In order to evaluate deployment performances at different pre-deformation temperatures, curves of position versus time were measured at the following pre-deformation temperatures:  $T_g-30^\circ\text{C}$ ,  $T_g-20^\circ\text{C}$ ,  $T_g-10^\circ\text{C}$ ,  $T_g$ ,  $T_g+10^\circ\text{C}$ . The deployment test of SMPC specimens was conducted at the  $T_g$  of SMPC ( $64^\circ\text{C}$ ) in a water bath. The original bent angle was selected as  $180^\circ$ .

As shown in Fig. 8, SMPC specimen also deploys relatively fast at elevated temperature in the initial 60 seconds, followed by deploying slowly then after. Fig. 9 presents the deployment ratio corresponding to different pre-deformation temperatures. It reveals that deployment ratio rises approximately linearly with the increase of pre-deformation temperatures. In additionally, from the comparison between Fig. 6 and Fig. 8, the curves are relatively dispersive in Fig. 6 than these in Fig. 8. It indicates that recovery temperature affects deployment performance more strongly than pre-deformation temperature does.

In conclusion, the deployment rate is relatively high in the initial stage, while decreases quickly beginning with a certain angle. The deployment ratio rises with the increase of deployment temperature and pre-deformation temperature. Moreover, the shape memory effect can also be observed at below  $T_g$  but still within the region of glass transition, although the deployment ratio is low. In the end, recovery temperature affects shape-recovery performance more strongly than pre-deformation temperature does.

### 3.3.3. Deployment ratio at different temperatures

In order to investigate the shape recovery ratio of SMPC at different temperatures, the test of shape recovery ratio versus the number of bending cycles was conducted at some different temperatures, namely  $T_g-30^\circ\text{C}$ ,  $T_g-20^\circ\text{C}$ ,  $T_g-10^\circ\text{C}$ ,  $T_g$ ,  $T_g+10^\circ\text{C}$ ,  $T_g+20^\circ\text{C}$  and  $T_g+30^\circ\text{C}$ . The original bent angle was selected as  $180^\circ$ . The temperature of pre-deformation of SMPC was set as  $T_g+20^\circ\text{C}$  in a water bath.

Fig. 10 shows that the recovery ratio decreases from 96% to 22% with the temperature decreasing from  $T_g+30^\circ\text{C}$  to  $T_g-20^\circ\text{C}$ . At  $T_g$ , the shape recovery ratio keeps within the range of 91~93%. At  $T_g-10^\circ\text{C}$ , the shape recovery ratio decreases from 72% to 57%. At  $T_g-20^\circ\text{C}$ , the shape recovery ratio decreases from 35% to 22%. In addition, the shape recovery effect can hardly be observed at below  $T_g-20^\circ\text{C}$ .

180

60

40

20

00

10

60

40

20

00

20

40

60

80

100

90

1578

Time (Seco)

It can be found that the shape recovery ratio of SMPC is high at/above  $T_g$ , which is above 90%. Moreover, the SMPC represents stable repeatability upon cycling. At above  $T_g$ , the shape recovery ratio against temperature shows a weak rising trend. The shape recovery behavior can also be observed within the range of  $T_g-20^\circ\text{C}$  to  $T_g$ , which demonstrates that the glass transition occurs in a continuous region ( $T_g-20^\circ\text{C}$  to  $T_g+20^\circ\text{C}$ , see Fig. 2). However, the shape recovery ratio drops sharply within this temperature range due to a relatively high stiffness of SMPC at the original stage of glass transition.

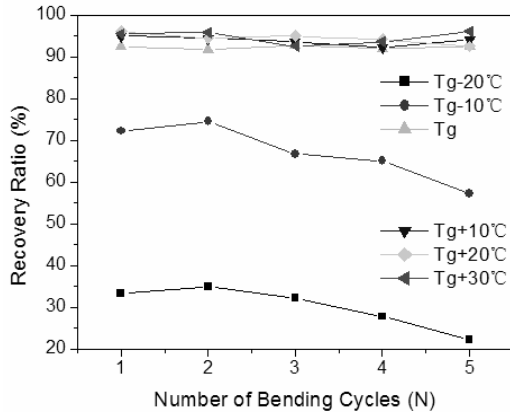


Fig. 10 Shape recovery ratio versus the number of bending cycles at different temperatures

### 3.3.4. Shape recovery ratio upon bending cycling

In order to evaluate the degradation of deployment, the relationship between shape recovery ratio and the number of bending cycles was tested at a bending angle of  $180^\circ$  at  $T_g+20^\circ\text{C}$  (see Fig. 11).

Fig. 11 shows that the recovery ratio decreases from 96% to 91% during first 50 bending cycles. For a single SMPC laminate, the shape recovery ratio decreases within a weak trend after some bending/deployment cycles. The shape recovery ratio becomes relatively stable after the 30th bending cycle, which keeps approximately at 90%. In addition, for the deployment process, SMPC deployed within two minutes approximately, wherein the recovery velocity in the beginning 30 seconds is relatively high.

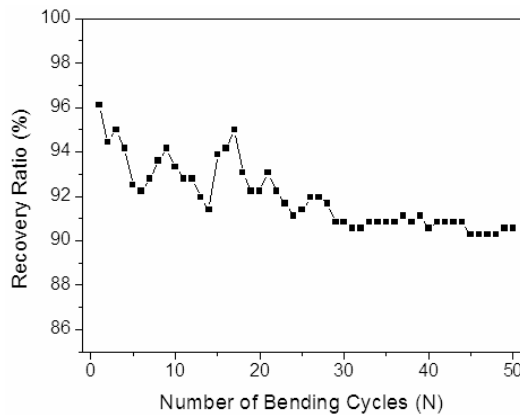


Fig. 11 Shape recovery ratio versus the number of

bending cycles at  $T_g +20^\circ\text{C}$

### 3.3.5. Residual angles at different original bending angles

The relationship between residual angle in recovered configuration and the number of bending cycles is obtained at the different original bending angles of  $45^\circ$ ,  $90^\circ$ ,  $135^\circ$  and  $180^\circ$  (see Fig. 12). Results indicate that the residual angle of the original bending angle of  $45^\circ$  is the lowest ( $3\sim 5^\circ$ ). The SMPC laminate with larger original bending angle results in a larger residual angle.

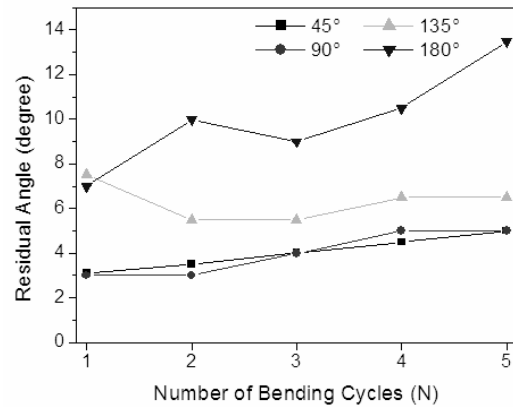


Fig. 12 Residual angle versus the number of bending cycles at different original bending angles

### 3.4. SMPC hinge

As shown in Fig.1, the prototype of SMPC hinge consists of two circular SMPC laminates. The length of each SMPC laminate is 100 mm. The radius of circular SMPC laminate is 125 mm with a thickness of 3 mm. The weight is 13.5 g for each piece of SMPC laminate.

Fig. 13 shows a deployment process of a prototype of solar arrays which is actuated by a SMPC hinge. Two surface heaters (nickel alloy heating element) are respectively bonded onto each inner surface of the two SMPC laminates. At a relatively soft state above  $T_g$ , the SMPC hinge is bent to  $180^\circ$  upon applying an external force. After fixing the shape at room temperature, the prototype of SMPC hinge is heated by passing an electrical current (voltage: 20V) through the surface-bonded heaters. The solar arrays, actuated by SMPC hinge, deploys from  $180^\circ$  to  $0^\circ$  in approximate 60 seconds. Moreover, the deployment velocity and shape recovery ratio are relatively stable during more than 10 thermomechanical cycles, which experiences stable deployment performances.

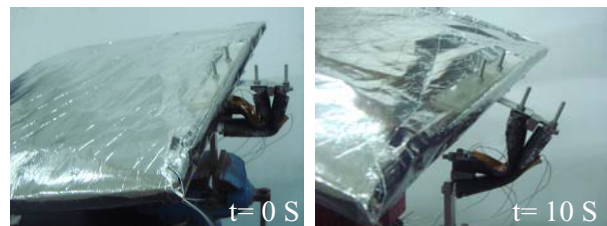




Fig.13 Process of deployment in a sequence of a prototype of a solar arrays actuated by SMPC hinge

#### 4. COCLUSIONS

(1) SMPC presents a higher glass transition temperature and higher storage modulus than those of pure SMP; (2) SMPC shows relatively high bending modulus before the glass transition in SMP, while exhibits low bending modulus within the range of glass transition in SMP; (3) Shape recovery velocity of SMPC rise remarkably with the increase of shape recovery temperature, while they increase in a weak trend with the increase of pre-deformation temperature; The shape recovery ratio of SMPC is above 90% at/above  $T_g$ , while drops sharply at below  $T_g$ . The shape recovery properties of SMPC depend strongly on the number of thermomechanical cycles, which become relatively stable after some packaging/deployment cycles. (4) A prototype of solar array actuated by SMPC hinge deploys from about  $180^\circ$  to  $0^\circ$  in one minute. This SMPC hinge performs good deployment performances during numerous thermomechanical cycles

#### REFERENCES

- [1] Marc Behl and Andreas Lendlein, "shape memory polymers", *Materials today*, Vol. 10, No. 4, 22-28 (2007)
- [2] Hayashi S. Properties and applications of polyurethane-series shape memory polymer. *International Progress in Urethanes*, 6, 90-115 (1993)
- [3] Tobushi H, Ito N, Hayashi S, Deformation in shape memory polymers of polyurethane series, *The 76th JSME Fall Annual Meeting*, 1:237-8 (1998)
- [4] Hayashi S. Properties and applications of polyurethane-series shape memory polymer. *International Progress in Urethanes*, 6, 90-115 (1993)
- [5] Gall, K., Dunn, M.L., et al., Shape memory polymer nanocomposites. *Acta Mater.* 50, 5115-5126 (2002)
- [6] Matthew C. Everhart, David M. Nickerson et al. High-Temperature Reusable Shape Memory Polymer Mandrels, *Smart Structures and Materials 2006: Industrial and Commercial Applications of Smart Structures Technologies*, Proc. of SPIE Vol. 6171, 61710K, (2006)
- [7] Jinsong Leng, Xin Lan et al., "Investigation of mechanical and conductive properties of shape memory polymer composite (SMPC) ", *Behavior and Mechanics of Multifunctional and Composite Materials 2007*, Proc. of SPIE Vol. 6526, 65262V (2007)
- [8] Ohki T, Ni QQ et al., Creep and cyclic mechanical properties of composites based on shape memory polymer, *Science and Engineering of Composite Materials*, 11 (2-3): 137-147 (2004)
- [9] Beavers, F., Gall, K., et al., "Developments in Elastic Memory Composite Materials for Spacecraft Deployable Structures", *Presented at the 2001 IEEE Aerospace Conference*, Big Sky, MT, March 10-17, IEEE Paper No. 01-3673 (2001)
- [10] Abrahamson, E. R., Lake, M. S, et al. Shape Memory Polymers for Elastic Memory Composites, *Presented at the 43rd AIAA/ASME/ ASCE/AHS/ASC SDM Conference*, April 22-25, 2002, Denver, CO, AIAA Paper No. 2002-1562 (2002)
- [11] Gall, K., Mikulas, M., Munshi, N.A., Carbon fiber reinforced shape memory polymer composites. *Journal of Intelligent Material Systems and Structures*. 11, 877-886 (2000)